

# Cortical Correlates of the Simulated Viewpoint Oscillation Advantage for Vection

Ramy Kirolos<sup>1,\*</sup>, Robert S. Allison<sup>1</sup> and Stephen Palmisano<sup>2,3</sup>

<sup>1</sup> Centre for Vision Research, York University, Toronto, ON, M3J 1P3, Canada

<sup>2</sup> Centre for Psychophysics, Psychophysiology, and Psychopharmacology

<sup>3</sup> School of Psychology, University of Wollongong, Wollongong, NSW, 2522, Australia

Received 30 January 2017; accepted 26 June 2017

---

## Abstract

Behavioural studies have consistently found stronger vection responses for oscillating, compared to smooth/constant, patterns of radial flow (the simulated viewpoint oscillation advantage for vection). Traditional accounts predict that simulated viewpoint oscillation should impair vection by increasing visual–vestibular conflicts in stationary observers (as this visual oscillation simulates self-accelerations that should strongly stimulate the vestibular apparatus). However, support for increased vestibular activity during accelerating vection has been mixed in the brain imaging literature. This fMRI study examined BOLD activity in visual (cingulate sulcus visual area — CSv; medial temporal complex — MT+; V6; precuneus motion area — PcM) and vestibular regions (parieto-insular vestibular cortex — PIVC/posterior insular cortex — PIC; ventral intraparietal region — VIP) when stationary observers were exposed to vection-inducing optic flow (i.e., globally coherent oscillating and smooth self-motion displays) as well as two suitable control displays. In line with earlier studies in which no vection occurred, CSv and PIVC/PIC both showed significantly increased BOLD activity during oscillating global motion compared to the other motion conditions (although this effect was found for fewer subjects in PIVC/PIC). The increase in BOLD activity in PIVC/PIC during prolonged exposure to the oscillating (compared to smooth) patterns of global optical flow appears consistent with vestibular facilitation.

## Keywords

Vection, visual–vestibular integration, fMRI, CSv, PIVC/PIC, oscillating/jitter advantage

---

\* To whom correspondence should be addressed. E-mail: ramykirollos@email.carleton.ca

## 1. Introduction

A variety of senses provide us with information about our active and passive self-motions through the environment. These include visual cues such as the global optic flow generated by self-motion (Gibson, 1966; Helmholtz, 1867), vestibular cues which signal active and passive head accelerations (Howard, 1982), as well as proprioceptive/somatosensory cues (Lishman and Lee, 1973). The importance of vision for self-motion perception is convincingly demonstrated by the fact that compelling visual illusions of self-motion can be induced in stationary observers (these illusions are commonly referred to as ‘vection’ — see Palmisano *et al.*, 2015). One familiar example of vection occurs when an individual on a stationary train watches a moving train on the adjacent track but feels instead that s/he is moving, despite being stationary (Mach, 1875, p. 127).

Much of the vection literature focuses on the sensory integration of visual and vestibular signals. During vection, conflicts are thought to arise between the visual (which is receiving stimulation indicating self-motion) and vestibular systems (which indicates that the observer is in fact stationary — see Reason, 1978). While the visual system is able to detect both constant velocity and accelerating motions (of the self and of objects — Previc and Ercoline, 2004), the vestibular system is only sensitive to passive and active accelerations of the head (Howard, 1982). Therefore, unlike the visual system, the vestibular system is unable to distinguish between moving at a constant velocity and remaining stationary (Lishman and Lee, 1973).

The magnitudes and durations of the visual–vestibular conflicts during vection have traditionally been thought to depend on the type of visually simulated self-motion (Oman, 1982). Specifically, smooth optic flow displays have been assumed to be low-conflict because they generally simulate self-motions with a constant speed and heading, and therefore do not correspond to movements that would generate sustained vestibular stimulation (except for transient signals when the display motion first starts and eventually ceases). By contrast, accelerating optic flow displays have been assumed to be high-conflict because they simulate self-motions with changes in speed and/or heading, which, during real motion, would strongly stimulate the vestibular system. Interestingly, a number of supposedly high conflict displays have been shown to generate more compelling vection than comparable low conflict displays as measured by vection magnitude ratings, vection onset latencies and vection durations (e.g., the simulated jitter and oscillation advantages for vection — Allison *et al.*, 2012; Palmisano *et al.*, 2000, 2008; see Palmisano *et al.*, 2011 for a review). For example, adding either simulated vertical viewpoint oscillation or camera shake to radial flow displays simulating constant velocity forward

self-motion has been shown to consistently increase the vection induced in stationary observers.

According to Brandt and colleagues (1998), one way for the brain to deal with visual–vestibular conflict during vection might be to inhibit vestibular processing thereby establishing visual dominance. In a positron emission tomography (PET) experiment, Brandt and colleagues exposed participants to visual displays intended to induce circular vection at a constant speed and had them rate their perceptions of self-motion on a scale from 1–5. Periods of circular vection correlated with heightened metabolic activity (signaled by  $H_2^{15}O$ -bolus levels) in medial parieto-occipital visual areas (as well as in the primary visual cortex) but reduced activity in the parieto-insular vestibular cortex compared to non-vection random-movement conditions. Specifically, Brandt and colleagues (1998) argued that these findings were evidence of reciprocal visual–vestibular inhibition during vection. This reciprocal visual–vestibular inhibition hypothesis was subsequently supported by a variety of follow-up studies also simulating constant speed self-motions (Brandt *et al.*, 2002; Deutschländer *et al.*, 2002, 2004; Dieterich *et al.*, 1998, 2003). For example, Deutschländer *et al.* (2004) compared metabolic activity patterns during circular and looming vection and concluded that both types of vection correlated with vestibular inhibition in parieto-insular regions.

On the other hand, Nishiike *et al.* (2002) examined brain activity during visually simulated self-motion via magnetoencephalography (MEG). Their displays simulated accelerating and constant velocity linear self-motions. During simulated self-acceleration (compared to constant velocity self-motion) they observed increased activation of posterior-insular regions classified as vestibular cortical areas. Although they did not measure vection directly (other than through informal reports), similar accelerating stimuli have repeatedly been shown to promote vection. Thus, Nishiike and colleagues' findings suggest that vection might be associated with increased neural activity in vestibular regions (i.e., vestibular facilitation, as opposed to vestibular inhibition, during visually induced illusory self-acceleration).

While Brandt *et al.* (1998) reported decreased cortical activity in vestibular cortical areas during constant vection, Nishiike *et al.* (2002) reported increased activity in vestibular cortical regions during accelerating self-motion displays. There are several possible explanations for the seemingly discrepant findings of both studies. First, Brandt and his colleagues used vection inducing displays that simulated constant speeds (thought to generate low sensory conflict), whereas Nishiike used displays that accelerated (thought to produce high conflict between visual and vestibular signals and corresponding cortical regions). Second, the techniques used for measuring vection differed in the two studies. Brandt *et al.* used a vection rating scale,

whereas Nishiike *et al.* used an indirect discrimination task combined with informal responses. Third, the studies used different brain imaging techniques (PET vs. MEG). Differences in the imaging parameters, underlying biophysics, as well as the spatial and temporal resolution of these techniques makes the results of these two studies difficult to compare and interpret.

Recent research on heading perception may also provide insights into the role of visual–vestibular interactions during (real/simulated) self-motion. According to Furlan and colleagues (2013), CSv activity strongly increases during visual display conditions which simulated horizontal oscillatory changes in heading direction (compared to activity in conditions which simulated constant heading). These authors suggest that CSv might play an important role in signaling changes in the direction of self-motion. Based on their findings we might expect to see increased activity in CSv during prolonged exposure to oscillatory (compared to smooth) self-motion displays. In other words, CSv activity might serve as a cortical correlate of the simulated viewpoint advantage for vection. However, to confirm this possibility we would need to re-examine whether these differences in neural activity persist under conditions that are more favorable to vection (infinite as opposed to limited object lifetimes, much longer durations of exposure to global motion, etc.). The experience of vection is quite different to heading perception. Vection involves the experience of compelling self-motion relative to an optic flow pattern and this experience of self-motion occurs in a distinct direction relative to said optic flow pattern. Vection is therefore a conscious illusion generally characterized by a finite latency (2–10 s) before it can be experienced. By contrast, heading perception only refers to the ability to determine the direction of implied self-motion from an optic flow pattern (Lepecq *et al.*, 2006). Because heading does not require the observer to experience that they are moving relative to a stationary scene (just that they can identify the direction in which the visual pattern signals self-motion), heading displays need not last as long as vection displays. As a result, many heading studies employ displays lasting a few milliseconds, or up to 2 s — such as the case in Furlan *et al.* (2013) whereas, vection displays usually last 20 s or longer because of its documented latency. An additional important distinction to make between vection and heading is that heading is generally regarded as being a prerequisite to vection — in other words, to experience vection, one must sense a direction in which they experience self-motion. However, the experience of vection is not necessary to determine heading direction. Heading and vection are similar in that they both are perceptual results of an optic flow pattern.

### 1.1. Current Experiment

The current fMRI study examined optic flow displays which simulated both constant speed (assumed low conflict) and accelerating (assumed high conflict) self-motions, allowing a direct evaluation of the effects of visual acceleration on self-motion related brain activity. Participants were given prolonged exposures to oscillating and smooth patterns of optic flow known to induce vection, as well as two suitable local motion control displays. The goals of this experiment were to: (1) search for neural correlates of the behaviourally observed oscillation advantage for vection; and (2) determine if there were consistent changes in BOLD signals in vestibular cortical regions during global motion displays, compared to local motion controls (the former types of displays being the more likely to induce vection).

To date, a number of cortical areas have been implicated in the processing of self-motion. Here we chose to examine activity in the medial temporal complex (MT+), the dorsomedial area (V6), the cingulate sulcus visual area (CSv), and precuneus motion area (PcM), as they have all been previously implicated in visual self-motion processing (e.g., Cardin and Smith, 2010, 2011; Kovacs *et al.*, 2008; Pitzalis *et al.*, 2013; Uesaki and Ashida, 2015; Wada *et al.*, 2016; Wall and Smith, 2008; only a subset of studies listed). We also examined activity in the vicinity of the human homologue of the parieto-insular vestibular cortex (PIVC) and the adjacent posterior insular cortex (PIC) as well as in the ventral intraparietal region (VIP) (see Note 1).

## 2. Methods

### 2.1. Participants

Eight volunteers from the York University community participated in the study (six males and two females). The mean age of participants was 31.5 years (SD = 8.4). Six participants were right-handed and two were left-handed. None reported any history of abnormal vestibular function. Seven participants had normal or corrected-to-normal vision. The eighth participant did not wear his habitual eyeglasses but could see the stimuli clearly at the near distance of the screen. Prior to the experiment, all participants provided their informed consent in accordance with a protocol approved by York University's Ethics Committee.

We ensured participants understood the task and that they all experienced vection during baseline (outside-of-scanner) testing conditions. Two additional participants were excluded from the study because they did not experience vection reliably during baseline testing.

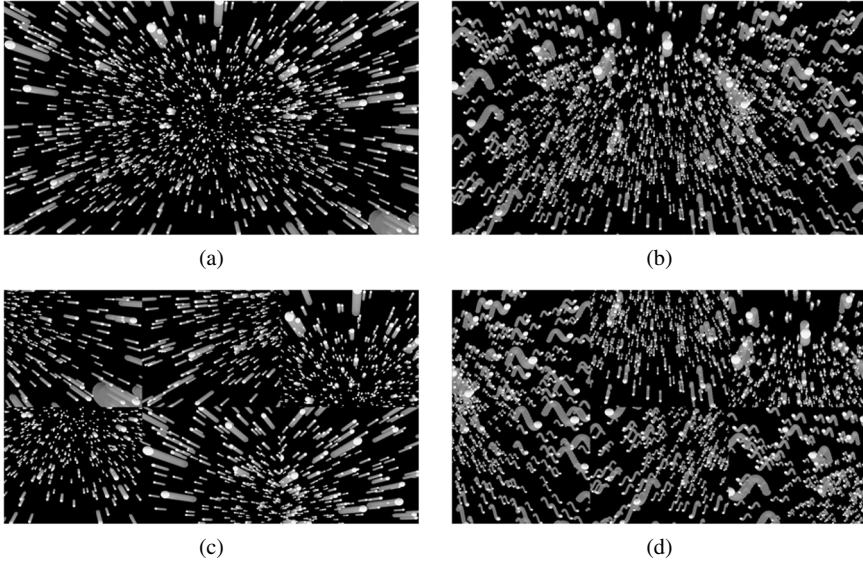


**Figure 1.** Schematic representations of the displays used. Top-left image represents the trajectories of the different spherical objects moving past the observer in the smooth global optic flow (Condition #1 — simulates purely forward self-motion). Top-right image represents trajectories of the spheres in the oscillating global optic flow (Condition #2). Bottom-left image represents the segmented and randomly re-ordered version used for the smooth local optic flow condition (Condition #3). Bottom-right image shows the segmented and randomly re-ordered version used for the oscillating local motion condition (Condition #4).

## 2.2. Visual Displays

Four different types of computer-generated visual display were presented (Fig. 1):

1. Smooth global optic flow: This display simulated smooth, constant-velocity forward self-motion. Consistent with the forward translation of the observer's simulated viewpoint, all of the elements in this display moved coherently in a radially expanding flow pattern (velocity varied according to simulated distance).
2. Oscillating global optic flow: This was similar to condition #1 with the addition of coherent, spinal-axis oscillatory motion of the observer's simulated viewpoint (i.e., vertical motion relative to the participant's body orientation, not to gravity).
3. Smooth local optic flow: This display was constructed by first dividing the coherent display from condition #1 into six sectors (3 by 2) and then randomly re-ordering the screen locations of these sectors.

4. Oscillating local optic flow: This condition was based on condition #2, but re-ordered in the same fashion as condition #3.

Each frame of the local motion image sequences was produced by segmenting the corresponding image in the global image sequence into six panels (three panels in the top half of the screen and three panels in the bottom half). To form the local motion image, the panels were reordered (scrambled) to scramble the global optic flow and no longer simulated forward self-motion.

Computer graphics animated displays were rendered using Pyglet ([www.pyglet.org](http://www.pyglet.org)), and depicted a virtual world 15 m wide, 15 m high, and 40 m deep. The computer graphics were rendered with a perspective projection appropriate for the distance and size of the display. In this virtual world there were 7000 evenly distributed textured blue spheres (diameter 15 cm each). In all displays the graphics camera translated through this virtual world of spheres at 0.08 meters per frame (60 Hz, 4.8 m/s). Sphere size, density, and velocity in the image varied as a function of simulated distance from the viewer according to perspective projection. As the viewer moved past a sphere in the simulation it was repositioned at the end of the virtual world so that the viewer never appeared to reach the 'end' of the volume. To prevent these spheres appearing suddenly and to avoid aliasing of very small spheres, a small amount of simulated fog was introduced to reduce visibility of the spheres at the extreme end of the visible volume (Note 2). All displays included a central, stationary, green fixation dot. The added display oscillation in conditions #2 and #4 was generated using the following formula for vertical displacement of the virtual camera:  $0.16 \times \sin(2\pi ft)$ , where 0.16 m/s was the peak up/down (spinal) speed of the virtual camera,  $f = 1.2$  Hz was the oscillation frequency and  $t$  was the time since the start of the motion (time progressed on each frame, that is, in discrete steps of 1/60 s). Displays began with a presentation of a 5-s static frame of the scene before simulated motion began. The simulated motion of objects in the scene lasted 20 s after which the vection display disappeared and then the response screen was presented.

### 2.3. Apparatus and Procedure

We used a Siemens 3-Tesla Magnetom Trio MRI Scanner (Erlangen, Germany) to collect anatomical and functional brain data. It was equipped with a 32-channel radio-frequency head coil. All displays were generated in real time on a T61 Lenovo ThinkPad laptop. The visual displays subtended  $36^\circ$  (horizontal) by  $27^\circ$  (vertical) at the 38 cm viewing distance and were presented via an Avotec projector onto a screen inside the scanner bore. The screen was reflected by a mirror (set at a  $45^\circ$  angle to the frontal plane) to form a frontal plane display for the supine subject.

During baseline testing, the subject lay supine on a massage table and the display of the laptop computer was mounted so that it was frontal at a distance of 38 cm from the participant's eyes. Participants viewed this display through a thick head-mounted frame, which approximated their field of view when the head coil was installed over their faces in the MRI. Baseline psychophysical measurements were obtained outside the scanner (in a nearby laboratory) before the MRI sessions to confirm that vection could be elicited reliably under physical conditions approximating the MRI setup, and to obtain measures of vection strength and onset. These measures were recorded with a Logitech gamepad. Participants were told to press and hold the right shoulder button on the gamepad when they experienced vection and to release this button when they did not experience vection. The button presses were time-stamped in an output file and later used to calculate the vection onset latency for each trial.

We used a magnitude estimation task to measure vection strength. To establish this scale, the first stimulus presented in every session was the smooth global optic flow display (i.e., condition #1). Participants were told to (a) monitor their sensation of self-motion during this display and to assign the sensation of vection experienced during this standard stimulus a strength of '50' on a 0–100 scale (the modulus) and (b) make subsequent estimates of vection strength proportionally relative to this modulus (Stevens, 1959). For instance, if the subject's experience of vection in a subsequent trial was twice as strong as the standard they were to report it as '100', whereas if vection was only half the strength of the standard they were to report it as '25'. For the baseline measures, participants entered these estimates with button presses on the gamepad at the end of each display.

#### 2.4. *Data Preprocessing*

A general linear model (GLM) was run in Fossil's (FSL) (5.0.1) FEAT functional MRI tool (v6.00). General linear model (GLM) is the modeling method used in FSL's FEAT and allows users to model the behavior of a voxel in a given time course and fit it to the real data.  $z$ -Scores are then automatically implemented by FEAT. The GLM in FEAT has many robust regressors built in to cancel noise created by head motion, physiological changes and magnetic properties of the scanner. Events of the experiment were categorized as six explanatory variables (EVs). These were the modulus stimulus, four experimental conditions (one EV each) and one EV for response intervals in which participants rated their sensation of vection after each trial. Static periods of each stimulus were used as the baseline in the GLM. EVs were represented in a raw text file making up the event-related design for the experiment. Conditions were labeled as 'ON' phases and static periods before the motion of stimuli began were treated as the 'OFF' phases/baseline. Inter-stimulus intervals (ISI) were 5 s long.

All data were spatially smoothed using estimates from random-field theory (RFT) at the full-width half maximum (FWHM) value of 5 mm of the Gaussian kernel smoothing process applied prior to processing the functional localizer data (Worsley *et al.*, 1992). Participants remained stationary throughout the experiment. However, brain images were motion corrected using the MCFLIRT tool set in FEAT to reduce the effect of any minor participant head motion (i.e., resulting from respiration). Non-brain tissue was filtered from the images using the BET brain extraction tool also built into FEAT. Functional data were overlaid on a standard 1 mm MNI brain, as well as each subject's structural image which also had a voxel size of  $1 \times 1 \times 1$  mm, and corrected for accidental head motion in 12 degrees of freedom. All data were modeled using a double-gamma hemodynamic response function (HRF).

### 2.5. MRI Scanning Parameters and Statistical Modeling

For the MRI sessions, the procedure was identical to that used for baseline testing except that the gamepad was not used to collect data. Instead, at the end of each display presentation participants provided their vection rating verbally which was then entered by the experimenter. For each participant, the experiment was divided into three functional runs in the MRI and contained 37 trials in total including the modulus display which was identical to the global smooth optic flow display. The modulus stimulus was presented at the beginning of the trials to set the standard for the vection magnitude judgements. Neither imaging nor psychophysical responses during this modulus stimulus were used in the analyses; it simply set the scale for magnitude estimates. The delay between the modulus stimulus and the first experimental trial was the same as the delay between experimental trials.

In experimental run 1, participants first viewed the modulus display followed by three repeats each of the four experimental display conditions (totaling 13 display presentations in run 1). The two following experimental runs did not contain a modulus display and therefore contained 12 displays each. Trials presented in each run were pseudo-randomized to control for adaptation effects.

Functional images were registered to a high-resolution T1-weighted MPRAGE sequence anatomical scan collected at the beginning of the scanning sessions. For the high-resolution anatomical scans, voxel size was  $1.0 \times 1.0 \times 0.95$  mm, TR = 1900 ms, TE = 2.52 ms, flip angle was  $9^\circ$  and FOV = 256 mm. Functional scans all shared the following parameters: T2\*-weighted, voxel size =  $3.0 \times 3.0 \times 3.5$  mm, TR = 2000 ms, TE = 30 ms, flip angle of  $90^\circ$  and FOV = 240 mm.

The three functional runs each subject underwent were concatenated in order to perform within subject region of interest (ROI) analyses. For these ROI analyses, masks of brain areas were created by registering a subject's brain

**Table 1.**

The left column contains brain regions of interest for our study. The right column shows the corresponding larger masks used

Brain region of interest	Talairach daemon label mask used
Medial temporal gyrus	Medial temporal region
Precuneus motion area	Precuneus
V6	Cuneus
Cingulate sulcus visual area	Cingulate gyrus
Parieto-insular vestibular cortex/posterior insular cortex	Insula
Ventral intraparietal region	Superior parietal lobe

with a 1-mm MNI standard brain in FSL View (version 5.0.1). Masks for areas V6, MT+, CSv, PcM, VIP and PIVC/PIC were based on Talairach Daemon Label atlas brain regions that corresponded to our brain region of interest. Masks were used to confine search areas, giving more statistical power but were loose, ensuring that they covered BOLD activity approximating each of these brain areas from the whole brain analysis of each subject. Table 1 displays the brain region of interest in the current study in the left column and its corresponding mask from Talairach Daemon Label atlas according to FSL View in the right column.

The contrast of primary interest was between oscillating global optic flow (Condition 2) and smooth global optic flow (Condition 1). In a secondary contrast, we combined these two global motion conditions (Conditions 1 and 2) and compared them with the two local motion conditions combined (Conditions 3 and 4) — this allowed the comparison of global and local motion BOLD activity. For all comparisons, voxels in all images were thresholded at a  $z$ -score of 2.3 or greater.

## 2.6. Functional Localizers

A series of functional localizer tests were used to identify areas MT, MST+ and V6. To functionally isolate the MT+ complex, we used the low-contrast radial rings display used by Pitzalis and colleagues (2010). We replicated Pitzalis *et al.*'s (2013) display to differentiate MT from MST+ using a patch of an expanding or contracting optic flow field. This stimulus is based on Dukelow and colleagues' (2001) stimulus and is hypothesized to selectively induce BOLD activity in the ipsilateral hemisphere in MST+, but induce BOLD activity in both MT and MST+ in the contralateral hemisphere. We also used Pitzalis *et al.*'s (2013) 'flow fields' stimulus to functionally localize V6.

### 2.7. Combined Anatomical and Functional Localizers

Anatomical localizers were used in identifying PIVC/PIC, VIP, and CSv because these are more difficult to isolate with functional techniques such as by visual stimulus presentation. Therefore, spatial coordinates of these areas from various sources were collected (Bremmer *et al.*, 2001; Cardin and Smith, 2010). Subsequently, we used our experimental vection stimuli to identify if these regions became functionally activated by our display. Our vection displays were successful in identifying these regions because coordinates that approximated those previously reported were found and fell within the confines of the masks. Though it must be acknowledged that a drawback of using anatomical localizers is their coarseness due to the inevitable variability between individual brains.

## 3. Results

### 3.1. Psychophysical Responses

Mean magnitude estimates for the baseline and MRI sessions are shown in Fig. 2 (Note 3). All behavioural analyses were performed in the SAS statistical software package (version 9.0). Participants reported experiencing vection on every global smooth and global oscillating trial tested during both baseline and MRI sessions (confirmed by their vection strength ratings obtained directly after each trial). A repeated-measures ANOVA found no significant differences between baseline vection magnitude ratings and those made during MRI sessions. Only the results of the analyses of the vection magnitude data obtained in the MRI sessions is provided below.

During MRI sessions, there was a significant effect of condition on vection magnitude ratings [ $F(3, 284) = 485.26, p < 0.05, R^2 = 0.84$ ] (Note 4).

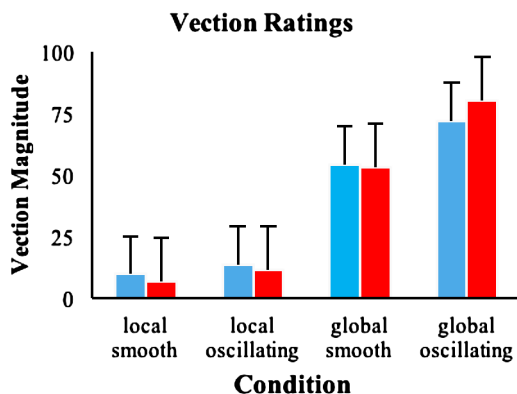


**Figure 2.** Mean vection magnitude estimates averaged across observers in each condition for baseline (blue) and MRI (red) sessions. Error bars indicate standard error of the mean.

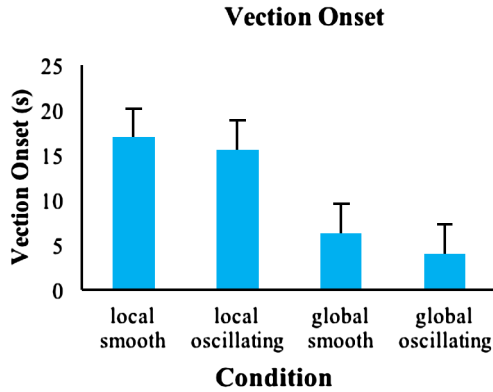


**Figure 3.** Mean vection onset latency averaged across observers in each condition during baseline sessions. Error bars indicate standard error of the mean.

Bonferroni-corrected pairwise  $t$ -tests showed that magnitude ratings differed significantly between all conditions. Consistent with previous research, post-hoc analyses revealed that: (1) oscillating global flow produced significantly stronger vection ratings than smooth global flow [ $t(7) = 14.51, p < 0.05$ ]; (2) Similarly, both global motion conditions produced stronger vection than their respective local motion conditions [ $t(7) = 21.09, p < 0.0001$  for global smooth compared with local smooth, and  $t(7) = 28.52, p < 0.0001$  for global oscillating compared with local oscillating]. While both of the local flow conditions produced weak vection ratings as expected, these were still significantly greater than zero suggesting that some vection was still being induced. Mean vection ratings were larger in the local oscillating condition than the local smooth condition although this difference was not significant in the baseline data.

Vection onset latency was only measured in the baseline sessions and was defined as time between the start of a trial and the first press of the response button that indicated that participants experienced vection. A repeated-measures ANOVA indicated a significant effect of condition on onset latency [ $F(3, 284) = 94.13, p < 0.05$ ]. Figure 3 shows that vection was obtained significantly more rapidly in the global oscillating ( $M = 4.0$  s) than in the global smooth condition ( $M = 6.28$  s) [ $t(7) = 2.92, p < 0.05$ ], consistent with the previously reported simulated viewpoint oscillation advantage for vection.

### 3.2. Localizer Data

Areas PcM, V6, MT+, MST+ and VIP did not show significant differences in BOLD activity in either of the contrasts examined. Areas CSv and PIVC/PIC were selectively responsive to global motion. Their results were analyzed in FSL FEAT (v6.00) and are presented below in MNI coordinates.

### 3.3. CSv Activity

CSv BOLD responses were found to be significantly greater during oscillating global optic flow relative to the smooth global optic flow for seven of our eight participants. BOLD activity in CSv was bilateral for this contrast and had an average  $z$ -score = 3.97,  $p = 0.02$  at  $x = 10$ ,  $y = -17$  and  $z = 41$  in the left hemisphere and an average  $z$ -score = 4.18,  $p < 0.02$  at  $x = -10$ ,  $y = -34$  and  $z = 37$  at in the right hemisphere in MNI coordinates. Data for subject 1 are shown in Fig. 4. Red–yellow colour gradients in these brain images represent significant  $z$ -scores (i.e., which were above the  $z = 2.3$  threshold (red) and became yellow as a function of  $z$ -scores surpassing this value).

The global motion versus local motion contrast collapsed oscillating and smooth global, as well as oscillating and smooth local, conditions together in order to compare differential BOLD effects for global and local motion patterns. This global motion versus local motion contrast indicated significantly greater CSv activation during global motion for five of our eight participants than for local motion. Results for subject 6 are shown below in Fig. 5.

BOLD signals in CSv were significantly greater for: (1) oscillating global flow compared to oscillating local flow for five of our eight participants (average  $z$ -score was 4.61,  $p < 0.05$ , at  $x = -17$ ,  $y = -33$ ,  $z = 39.5$  in the left hemisphere; average  $z$ -score of 4.75,  $p < 0.05$  at  $x = 11.6$ ,  $y = -14.7$ ,  $z = 40$  in the right hemisphere), and (2) oscillating global flow compared to smooth local flow for all eight participants (average  $z$ -score was 4.03,  $p < 0.05$ , at  $x = -9.9$ ,  $y = -30.1$ ,  $z = 36.7$  in the left hemisphere; average  $z$ -score of

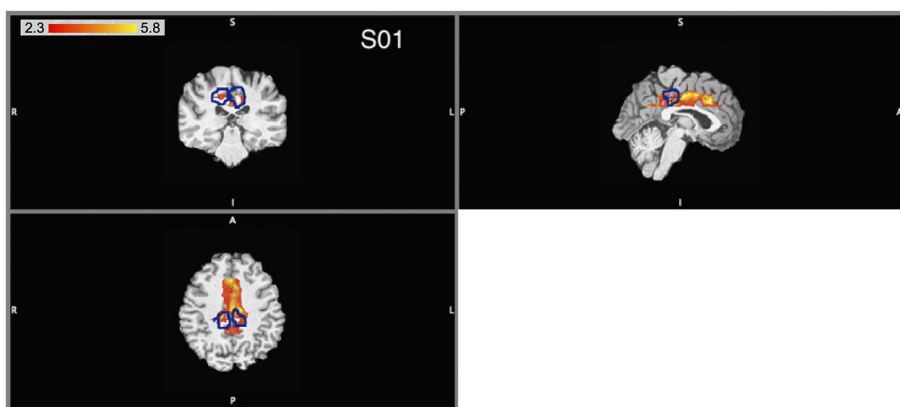


**Figure 4.** BOLD activity for the oscillating global > smooth global contrast in CSv for subject 1. The blue outlines indicate an approximation of area CSv in subject 1. Above threshold BOLD activity is represented by the red–yellow colour gradient and ranges from  $Z = 2.3$  (red) to 5.8 (yellow).

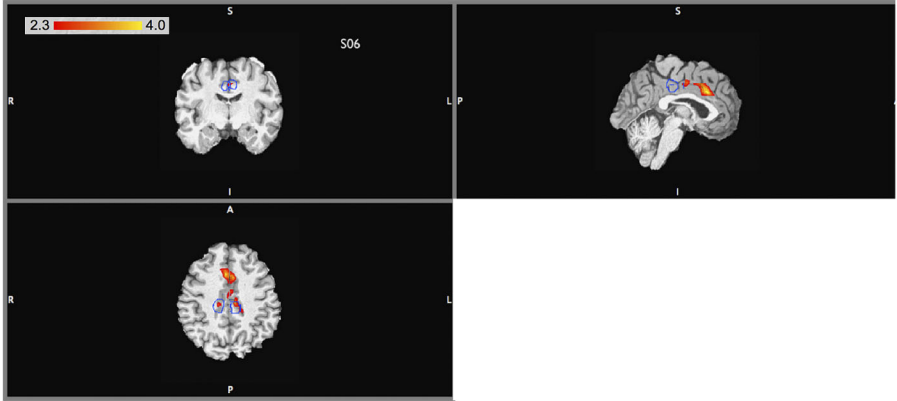


**Figure 5.** CSv activity for the global motion > local motion contrast for subject 6. The blue outlines indicate an approximation of area CSv in the subject. Above threshold BOLD activity is represented by the red–yellow colour gradient and ranges from  $Z = 2.3$  (red) to 4.0 (yellow).

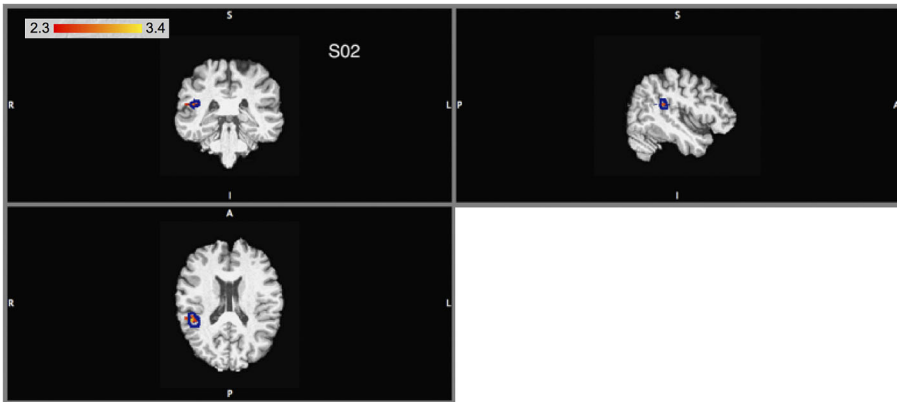


**Figure 6.** PIVC/PIC activity for the oscillating global > smooth global contrast in subject 2. The blue outline represents approximate location of participant’s PIVC/PIC. Above threshold BOLD activity is represented by the red–yellow colour gradient and ranges from  $Z = 2.3$  (red) to 3.4 (yellow).

3.52,  $p < 0.05$  at  $x = 9.5$ ,  $y = -37$ ,  $z = 31.7$  in the right hemisphere). However, BOLD responses for smooth global flow and smooth local flow were not significantly different.

### 3.4. PIVC/PIC Activity

In PIVC/PIC we found significantly larger BOLD responses for oscillating global flow compared to smooth global flow for five of our eight participants bilaterally. In the left hemisphere this resulted in an average  $z$ -score of 5.07,  $p < 0.05$ , at  $x = 44$ ,  $y = -28.8$ , and  $z = 17$ . In the right hemisphere the

average  $z$ -score was 5.01,  $p < 0.05$  at  $x = 51.7$ ,  $y = -35$  and  $z = 20$ . An illustration of this result for participant 2 is shown in Fig. 6.

No significant differences were found for contrasts comparing BOLD activity for global motion and local motion displays in PIVC/PIC.

## 4. Discussion

Behaviourally, vection magnitude ratings were significantly larger for oscillating global flow displays than for smooth global flow displays. Vection onset times for this oscillating global flow were also significantly shorter than those for the smooth global flow (measured during baseline testing only), consistent with the notion that stronger vection displays yield quicker vection percepts, therefore replicating the simulated viewpoint oscillation advantage for vection (e.g., Palmisano *et al.*, 2011).

More importantly, we appear to have identified two neural correlates of this oscillation advantage for vection using fMRI. We found significantly larger BOLD responses in both PIVC/PIC and CSv during oscillating global flow (compared to smooth global flow). We will discuss the optic flow based activity in these two ROIs in more detail below.

### 4.1. CSv

When taken together with previous findings, the current results suggest that CSv plays an important role in signaling changes in the direction of self-motion. During prolonged exposures to global motion, we found that CSv activity was greater for displays which induced vertically oscillating vection in depth compared to displays which simulated smooth vection in a constant direction. These findings appear quite consistent with those of an earlier study by Furlan *et al.* (2013) which did not induce vection. They found that CSv activity was greater during visually simulated horizontal oscillations in heading direction compared to simulated constant heading. It is, as one reviewer pointed out, therefore possible that BOLD responses in our experiment correlated with the changes in heading. If this was the case then our results demonstrate that this increased CSv activity persists for oscillating (i.e., heading change) conditions when participants actually feel that they are moving.

In the case of fMRI, Pitzalis *et al.* (2013) have argued that we can only be sure that we are actually examining the cortical activity related to self-motion processing/perception when the physically stationary observer is actually experiencing vection. Since Furlan *et al.*'s motion stimuli only lasted 2 s, their dots did not loom and had limited lifetimes (500 ms), it is unlikely that their displays induced any vection. By contrast, we know that our subjects were experiencing vection in *all* global smooth and global oscillating conditions inside the scanner (as vection strength ratings were obtained after every trial).

Our study used longer and larger exposures to the visual motion of looming, persisting objects. Additionally, we looked at global vertical oscillation when travelling through a 3-D cloud, whereas Furlan *et al.*, looked at global horizontal oscillation when travelling over a ground plane. As stated above, our CSv results appear to corroborate those of Furlan and colleagues. However, if we happen to be replicating their original effect, we also have shown that such activity generalizes considerably to much longer durations of motion stimulation, to conditions that actually induce vection, and to different simulated environments (i.e., looming and persisting objects arranged in 3D clouds).

It should be noted that Wada and colleagues (2016) have found evidence of increased BOLD activity in CSv for optic flow displays simulating smooth forward self-motion. Their experiment used a rapid event-related design that constrained displays of forward self-motion stimuli to 3 s durations. Despite these brief presentations, they found a significantly larger BOLD response for the displays simulating forwards self-motion compared to the random dot motion controls in CSv. Thus, while CSv appears to prefer simulated self-motions that change in direction, this region also responds to self-motions with a constant heading.

#### 4.2. PIVC/PIC

BOLD activity in vestibular region PIVC/PIC was greater for oscillating global flow than for smooth global flow in our study. These findings do not appear to support the notion of vestibular inhibition during vection (Brandt *et al.*, 1998), as conditions in our experiment with (expected) higher visual–vestibular conflict actually generated more BOLD activity in vestibular–cortical area PIVC/PIC. Instead our PIVC/PIC findings appear to instead support the vestibular facilitation hypothesis suggested by Nishiike and colleagues (2002). It should be noted that what we here refer to as PIVC/PIC, could include what Frank and colleagues (2016) have described as area PIC. Our anatomical localizer was not sufficiently precise to distinguish PIVC and PIC. In Frank *et al.* (2016), PIVC became active during caloric irrigations and cortical BOLD activity in this region was suppressed when visual displays were presented alone. Interestingly, an adjacent insular region — the posterior insular cortex (PIC) — was not only active during caloric irrigation alone, but remained active during purely visual trials signaling self-motion. It is possible therefore that the increased PIVC/PIC activation in our study actually reflected increased visual activity in PIC (Note 5). It is also possible that Brandt and colleagues (1998) might have functionally localized PIVC/PIC in their study, whereas Nishiike and colleagues (2002) instead identified PIC. This could be another possible explanation for the apparent discrepancy in their findings of vestibular inhibition and vestibular facilitation (respectively) during exposure to self-motion consistent optic flow.

In general, our PIVC/PIC findings appear consistent with a recent study by Uesaki and Ashida (2015) that reported increased BOLD activity in this region during vection. In their experiment, Uesaki and Ashida used 16 s binocular stimuli consisting of spiral optic flow patterns either with or without radial speed gradients. Optic flow patterns with speed gradients were expected to induce forward and backward vection (with rotation) while the flow without speed gradients would have been inconsistent with vection. BOLD activity observed in PIVC/PIC was larger during vection which appears to be inconsistent with Brandt and colleagues' (1998) findings. Uesaki and Ashida provide two possible reasons for their apparently discrepant results: (1) Brandt and colleagues simulated self-motion about only a single axis (i.e., circular vection), whereas they simulated self-motions about multiple axes with their spiral flow; (2) Brandt and colleagues used constant-motion displays whereas Uesaki and Ashida used stimuli that visually signaled self-acceleration and linear direction changes. Our current results, which demonstrate increased PIVC/PIC activity for oscillating global flow, directly support Uesaki and Ashida's latter explanation. Interestingly, in our study, PIVC/PIC did not show a difference in BOLD activation when oscillating global optic flow was compared with either of the local motion control conditions, suggesting that PIVC/PIC might not correlate exclusively with vection processing. In all, our findings appear to suggest increased PIVC/PIC BOLD activity during high-conflict vection displays.

An alternative but unlikely reason for the observed increases in vestibular cortical activity during our study and the study by Uesaki and Ashida (2015) but not the Brandt *et al.* (1998) study was magnetically induced vestibular stimulation. Magnetically induced vestibular stimulation has been previously reported in high magnetic fields (Roberts *et al.*, 2011). However, any such effects should have been weak in the relatively modest field (3T) scanner used in our experiment and there would be no reason to expect that these peripheral vestibular effects would vary systematically with our visual stimuli (i.e., any magnetically induced vestibular stimulation should have been constant for each observer throughout the experiment). Thus, while such magnetic effects could (in principle) underlie our findings of both significant BOLD responses in 'vestibular' areas and unexpected vection during displays that produce no or weak vection outside the scanner (such as our local motion control displays and the 'no speed gradient' displays of Uesaki and Ashida), they cannot explain selective PIVC/PIC activity for our high-conflict vection-inducing displays.

In our study, PIVC/PIC showed greater BOLD activity for oscillating global flow than for smooth global flow. This BOLD activity is thought to be excitatory rather than inhibitory. Though there is some debate regarding BOLD signals reflecting excitatory or inhibitory activity in the cortex, many studies have reported a preponderance for excitatory BOLD responses. For instance,

Lee *et al.* (2010) used a combination of high-field fMRI and optogenetic stimulation in mice motor cortices to investigate if BOLD activity was excitatory or inhibitory. In traditional M1 stimulation trials, they found excitatory BOLD activity. Moreover, electrode responses in the thalamus indicated excitatory cell activity, correlating with the region's positive BOLD response. Lee and colleagues state that the excitatory activity noted in M1 corresponds with the dynamics of a typical BOLD-fMRI stimulus evoked response, suggesting that BOLD activity is predominantly excitatory. Atwell and Iadecola (2002) also report excitatory activity and report that inhibitory neurons are much rarer in the cortex than excitatory neurons (Abeles, 1991; Braitenberg and Schüz, 1998). In a study by Waldvogel *et al.* (2000) comparing BOLD signals of excitatory and inhibitory neurons in the motor cortex, the authors argue that BOLD signal increase is generally associated with excitatory activity rather than inhibitory neural activity. This is because authors found no change in BOLD signals accompanying firing of inhibitory neurons, but observed a notable BOLD signal change during excitatory neuron activity. Waldvogel and colleagues' results suggest that BOLD signal generally reflects excitatory activity. Therefore, though studies have suggested that BOLD activity may reflect LFP (Logothetis, 2008), inhibitory activity may be negligible, and much rarer than excitatory activity.

#### 4.3. *Other ROIs*

Our results differed from several previous studies that suggested a role in vection for regions V6 (Pitzalis *et al.*, 2013; Uesaki and Ashida, 2015; Wada *et al.*, 2016), VIP (Bremmer *et al.*, 2001), PcM (Billington *et al.*, 2013) and the MT+ complex (Miyazaki *et al.*, 2015). Unlike these studies, we did not find selective BOLD activation in these regions for global (analogous to vection-compatible) compared to local (vection-incompatible) optic flow in our experiment. One likely explanation for these apparent discrepancies was our use of vertically oscillating (global and local) optic flow displays. To our knowledge brain activity associated with self-motion perception has not been examined in this context before. Some studies citing increased V6 activity during coherent compared to random motion did not explicitly measure vection (as noted by Pitzalis *et al.*, 2013). Similarly, while VIP has been shown to respond to coherent optic flow displays (Bremmer *et al.*, 2001; Cardin and Smith, 2010; Smith *et al.*, 2012) these studies have mainly focused on heading estimation (Billington *et al.*, 2013; Fischer *et al.*, 2012; Furlan *et al.*, 2013) or did not explicitly measure vection. In the current experiment, the individual spherical objects in the 3D cloud had an infinite lifetime (they were visible as long as they were on the screen and as long as the display lasted). On the other hand, dot lifetime was only 133 ms in the Wall and Smith (2008) study. Wall and Smith reported

strong VIP activity for their egomotion compatible (global spiral motion) stimuli. While their displays lasted 5 s, the use of limited dot lifetimes may have delayed/prevented vection onset. This may perhaps explain why VIP activity was not observed in the current study, but was reported in Wall and Smith. Alternatively, it might have arisen due to differences in flow type (radial versus spiral) display size ( $36 \times 27$  degrees versus  $20 \times 20$  degrees) or object type (looming sphere versus dot). These results and ours can be reconciled if Wada *et al.* (2016) are correct in their interpretation that V6 (and presumably VIP as well) is responsive to coherent flow but does not specifically correlate with self-motion perception. Similarly, Wada *et al.* (2016) found that MT+ responded indiscriminately to various types of visual motion patterns, and thus it is not surprising that we found similar MT+ activation in vection compatible and incompatible conditions, despite previous reports of selective sensitivity to coherent motion in this area (Huk and Heeger, 2002; Tootell *et al.*, 1995; Watson *et al.*, 1993; Zeki *et al.*, 1991). However, our results still appear to be at odds with those of Uesaki and Ashida (2015) in terms of V6 activity (since they measured vection and reported correlated BOLD activity in V6).

Our results also appear to provide little support for the notion of increased metabolic activity for area PcM during global compared to local motion displays, contrary to findings by Billington and colleagues (2013), Cardin and Smith (2010) and Wada and colleagues (2016). All three studies found increased PcM activity during coherent optic flow versus random motion displays. It is generally thought that PcM is related to cognitive aspects of self-motion (Wolbers *et al.*, 2007, 2008) and less directly related to self-motion perception. Therefore, it appears the role of PcM in self-motion remains mixed in light of some of the recent studies mentioned above.

## 5. Conclusions

In summary, we set out to identify visual and vestibular brain regions that functionally correlate with vection magnitude. Specifically, we looked for neural correlates of the behaviourally observed oscillation advantage for vection. Consistent with the behavioural response, oscillating global flow patterns induced stronger BOLD activation in CSv and PIVC/PIC compared to weaker vection-inducing displays. The increased activation in area PIVC/PIC occurs despite expectations of sustained visual–vestibular conflict with the oscillating stimulus; thus, our results are consistent with the vestibular facilitation hypothesis. Vection inducing stimuli appear to elicit corollary responses in polysensory and vestibular areas consistent with the visually-signaled self-motion. These responses may play a determining role in the conscious perception of vection and in the integration of visual and vestibular self-motion signals during real-motion.

### *Acknowledgements*

This research was supported by the National Science and Engineering Research Council of Canada's CREATE program for applications in vision science and the Centre for Vision Research, York University.

### *Conflict of Interest*

The authors declare that they have no conflict of interest.

### **Notes**

1. Because PIVC is suppressed by visual stimulation that causes vection (Brandt *et al.*, 1998) but PIC is visually responsive (Frank *et al.*, 2016), it is likely that any excitatory visual or vection-related activity seen in this vicinity arises in PIC. However we did not separate the two regions with localizers, so such activity will be labelled PIVC/PIC.
2. Due to perspective projection, the diameter of the images of the spheres varied widely: from  $0.21^\circ$  to  $10.9^\circ$  at 40 m and 0.78 m (the closest distance where the center of a sphere could be seen in the image), respectively. Similarly, image speed varied with distance and eccentricity as in the natural world, for example from 0.05 deg/s for a central sphere at 40 m to 113 deg/s for sphere at 0.78 m going off the side of the display during the smooth global optic flow display.
3. Vection Magnitude ratings for the Global Smooth condition were slightly greater than 50 ( $M = 53$  in baseline sessions and  $M = 52$  in fMRI sessions). The mean ratings approximate the definition but due to variability, are not expected to be exactly 50.
4. Note that the behavioural vection strength ratings recorded in these scanning sessions were highly correlated with those recorded in the baseline testing sessions in all trials across participants (Pearson correlation = 0.87).
5. However, if the region we localized in the current study was in fact PIC and not PIVC, we would expect activation in this region for all global > local contrasts in our study, but this was not the case.

### **References**

- Abeles, M. (1991). *Corticonics: Neural Circuits of the Cerebral Cortex*. Cambridge University Press, Cambridge, UK.

- Allison, R. S., Zacher, J. E., Kirolos, R., Guterman, P. S. and Palmisano, S. (2012). Perception of smooth and perturbed vection in short-duration microgravity, *Exp. Brain Res.* **223**, 479–487.
- Attwell, D. and Iadecola, C. (2002). The neural basis of functional brain imaging signals, *Trends Neurosci.* **25**, 621–625.
- Billington, J., Wilkie, R. M. and Wann, J. P. (2013). Obstacle avoidance and smooth trajectory control: neural areas highlighted during improved locomotor performance, *Front. Behav. Neurosci.* **7**, 9. DOI:10.3389/fnbeh.2013.00009.
- Braitenberg, V. and Schüz, A. (1998). *Cortex: Statistics and Geometry of Neuronal Connectivity*, 2nd edn. Springer-Verlag, Heidelberg, Germany.
- Brandt, S. A., Brocke, J., Roricht, S., Ploner, C. J., Villringer, A. and Meyer, B. U. (2002). In vivo assessment of human visual system connectivity with transcranial electrical stimulation during functional magnetic resonance imaging, *Neuroimage* **14**, 366–375.
- Brandt, T., Bartenstein, P., Janek, A. and Dieterich, M. (1998). Reciprocal inhibitory visual–vestibular interaction. Visual motion stimulation deactivates the parieto-insular vestibular cortex, *Brain* **121**, 1749–1758.
- Bremmer, F., Schlack, A., Shah, N. J., Zafiris, O., Kubischik, M., Hoffmann, K. and Fink, G. R. (2001). Polymodal motion processing in posterior parietal and premotor cortex: a human fMRI study strongly implies equivalencies between humans and monkeys, *Neuron* **29**, 287–296.
- Cardin, V. and Smith, A. T. (2010). Sensitivity of human visual and vestibular cortical regions to egomotion-compatible visual stimulation, *Cereb. Cortex* **20**, 1964–1973.
- Cardin, V. and Smith, A. T. (2011). Sensitivity of human visual cortical area V6 to stereoscopic depth gradients associated with self-motion, *J. Neurophysiol.* **106**, 1240–1249.
- Deuschländer, A., Bense, S., Stephan, T., Schwaiger, M., Brandt, T. and Dietrich, M. (2002). Sensory systems interactions during simultaneous vestibular and visual stimulation in PET, *Hum Brain Mapp.* **16**, 92–103.
- Deuschländer, A., Bense, S., Stephan, T., Schwaiger, T., Dieterich, M. and Brandt, T. (2004). Roll vection versus linear vection: comparison of brain activations in PET, *Hum Brain Mapp.* **21**, 143–153.
- Dieterich, M., Bucher, S. F., Seelos, K. C. and Brandt, T. (1998). Horizontal or vertical optokinetic stimulation activates visual motion-sensitive ocular-motor and vestibular cortex areas with right hemispheric dominance. An fMRI study, *Brain* **121**, 1479–1495.
- Dieterich, M., Bense, S., Stephan, T., Yousry, T. A. and Brandt, T. (2003). fMRI signal increases and decreases in cortical areas during small-field optokinetic stimulation and central fixation, *Exp. Brain Res.* **148**, 117–127.
- Dukelow, S. P., DeSouza, J. F., Culham, J. C., Van den Berg, A. V. and Menon, R. S. (2001). Distinguishing subregions of the human MT+ complex using visual fields and pursuit eye movements, *J. Neurophysiol.* **86**, 1991–2000.
- Fischer, E., Bühlhoff, H. H., Logothetis, N. K. and Bartels, A. (2012). Visual motion responses in the posterior cingulate sulcus: a comparison to V5/MT and MST, *Cereb. Cortex* **22**, 865–876.
- Frank, S. M., Wirth, A. M. and Greenlee, M. W. (2016). Visual–vestibular processing in the human Sylvian fissure, *J. Neurophysiol.* **116**, 263–271.

- Furlan, M., Wann, J. P. and Smith, A. T. (2013). A representation of changing heading direction in human cortical areas pVIP and CSv, *Cereb. Cortex* **24**, 2848–2858.
- Gibson, J. J. (1966). *The Senses Considered as Perceptual Systems*. Houghton Mifflin, Boston, MA, USA.
- Helmholtz, H. (1867). *Handbuch der Physiologischen Optik*, Vol. 9. Leopold Voss, Leipzig, Germany.
- Howard, I. (1982). *Human Visual Orientation*. Wiley, New York, NY, USA.
- Huk, A. C. and Heeger, D. J. (2002). Pattern-motion responses in human visual cortex, *Nat. Neurosci.* **5**, 72–75.
- Kovács, G., Raabe, M. and Greenlee, M. W. (2008). Neural correlates of visually induced self-motion illusion in depth, *Cereb. Cortex* **18**, 1779–1787.
- Lee, J. H., Durand, R., Gradinaru, V., Zhang, F., Goshen, I., Kim, D. S. and Deisseroth, K. (2010). Global and local fMRI signals driven by neurons defined optogenetically by type and wiring, *Nature* **465**(7299), 788–792.
- Lepecq, J. C., De Waele, C., Mertz-Josse, S., Teyssèdre, C., Huy, P. T., Baudonnière, P. M. and Vidal, P. P. (2006). Galvanic vestibular stimulation modifies vection paths in healthy subjects, *J. Neurophysiol.* **95**, 3199–3207.
- Lishman, J. R. and Lee, D. N. (1973). The autonomy of visual kinaesthesia, *Perception* **2**, 287–294.
- Logothetis, N. K. (2008). What we can do and what we cannot do with fMRI, *Nature* **453**(7197), 869–878.
- Mach, E. (1875). *Grundlinien der Lehre von den Bewegungsempfindungen*. Engelmann, Leipzig, Germany.
- Miyazaki, J., Yamamoto, H., Ichimura, Y., Yamashiro, H., Murase, T., Yamamoto, T. and Higuchi, T. (2015). Inter-hemispheric desynchronization of the human MT+ during visually induced motion sickness, *Exp. Brain Res.* **233**, 2421–2431.
- Nishiike, S., Nakagawa, S., Nakagawa, A., Uno, A., Tonoike, M., Takeda, N. and Kubo, T. (2002). Magnetic cortical responses evoked by visual linear forward acceleration, *Neuroreport* **13**, 1805–1808.
- Oman, C. H. (1982). A heuristic mathematical model for the dynamics of sensory conflict and motion sickness, *Acta Oto-Laryngologica* **94**, 4–44.
- Palmisano, S., Gillam, B. J. and Blackburn, S. G. (2000). Global-perspective jitter improves vection in central vision, *Perception* **29**, 57–67.
- Palmisano, S., Allison, R. S. and Pekin, F. (2008). Accelerating self-motion displays produce more compelling vection in depth, *Perception* **37**, 22–33.
- Palmisano, S., Allison, R. S., Kim, J. and Bonato, F. (2011). Simulated viewpoint jitter shakes sensory conflict accounts of vection, *See. Perceiv.* **24**, 173–200.
- Palmisano, S., Allison, R. S., Schira, M. M. and Barry, R. J. (2015). Future challenges for vection research: definitions, functional significance, measures and neural bases, *Front. Psychol.* **6**, 193. DOI:10.3389/fpsyg.2015.00193.
- Pitzalis, S., Sereno, M. I., Committeri, G., Fattori, P., Galati, G., Patria, F. and Galletti, C. (2010). Human V6: the medial motion area, *Cereb. Cortex* **20**, 411–424.
- Pitzalis, S., Sdoia, S., Bultrini, A., Committeri, G., Di Russo, F., Fattori, P., Galletti, C. and Galati, G. (2013). Selectivity to translational egomotion in human brain motion areas, *PLoS One* **8**, e60241. DOI:10.1371/journal.pone.0060241.

- Previc, F. H. and Ercoline, W. R. (Eds) (2004). *Spatial Disorientation in Aviation*, Vol. 203. AIAA, Reston, VA, USA.
- Reason, J. T. (1978). Motion sickness adaptation: a neural mismatch model, *R. Soc. Med.* **71**, 819–829.
- Roberts, D. C., Marcelli, V., Gillen, J. S., Carey, J. P., Della Santina, C. C. and Zee, D. S. (2011). MRI magnetic field stimulates rotational sensors of the brain, *Curr. Biol.* **21**, 1635–1640.
- Smith, A. T., Wall, M. B. and Thilo, K. V. (2012). Vestibular inputs to human motion-sensitive visual cortex, *Cereb. Cortex* **22**, 1068–1077. DOI:10.1093/cercor/bhr179.
- Stevens, S. S. (1959). Cross-modality validation of subjective scales for loudness, vibration, and electric shock, *J. Exp. Psychol.* **57**, 201–209.
- Tootell, R. B., Reppas, J. B., Kwong, K. K., Malach, R., Born, R. T., Brady, T. J. and Belliveau, J. W. (1995). Functional analysis of human MT and related visual cortical areas using magnetic resonance imaging, *J. Neurosci.* **15**, 3215–3230.
- Uesaki, M. and Ashida, H. (2015). Optic-flow selective cortical sensory regions associated with self-reported states of vection, *Front. Psychol.* **6**, 755. DOI:10.3389/fpsyg.2015.00775.
- Wada, A., Sakano, Y. and Ando, H. (2016). Differential responses to a visual self-motion signal in human medial cortical regions revealed by wide-view stimulation, *Front. Psychol.* **7**, 309. DOI:10.3389/fpsyg.2016.00309.
- Waldvogel, D., Van Gelderen, P., Muellbacher, W., Ziemann, U., Immisch, I. and Hallett, M. (2000). The relative metabolic demand of inhibition and excitation, *Nature* **406**(6799), 995–998.
- Wall, M. B. and Smith, A. T. (2008). The representation of egomotion in the human brain, *Curr. Biol.* **18**, 191–194.
- Watson, J. D., Myers, R., Frackowiak, R. S., Hajnal, J. V., Woods, R. P., Mazziotta, J. C. and Zeki, S. (1993). Area V5 of the human brain: evidence from a combined study using positron emission tomography and magnetic resonance imaging, *Cereb. Cortex* **3**, 79–94.
- Wolbers, T., Wiener, J. M., Mallot, H. A. and Büchel, C. (2007). Differential recruitment of the hippocampus, medial prefrontal cortex, and the human motion complex during path integration in humans, *J. Neurosci.* **27**, 9408–9416.
- Wolbers, T., Hegarty, M., Büchel, C. and Loomis, J. M. (2008). Spatial updating: how the brain keeps track of changing object locations during observer motion, *Nat. Neurosci.* **11**, 1223–1230.
- Worsley, K. J., Evans, A. C., Marrett, S. and Neelin, P. (1992). A three-dimensional statistical analysis for CBF activation studies in human brain, *J. Cereb. Blood Flow Metab.* **12**, 900–918.
- Zeki, S., Watson, J. D., Lueck, C. J., Friston, K. J., Kennard, C. and Frackowiak, R. S. (1991). A direct demonstration of functional specialization in human visual cortex, *J. Neurosci.* **11**, 641–649.